Laboratori Nazionali di Frascati

LNF-92/084 (P)
4 Novembre 1992

A. Courau, G. Pancheri:

TWO PHOTON CONTRIBUTION TO THE PROCESS $e^+e^- \to e^+e^- \pi\pi$

Contribution to the DAΦNE Physics Handbook

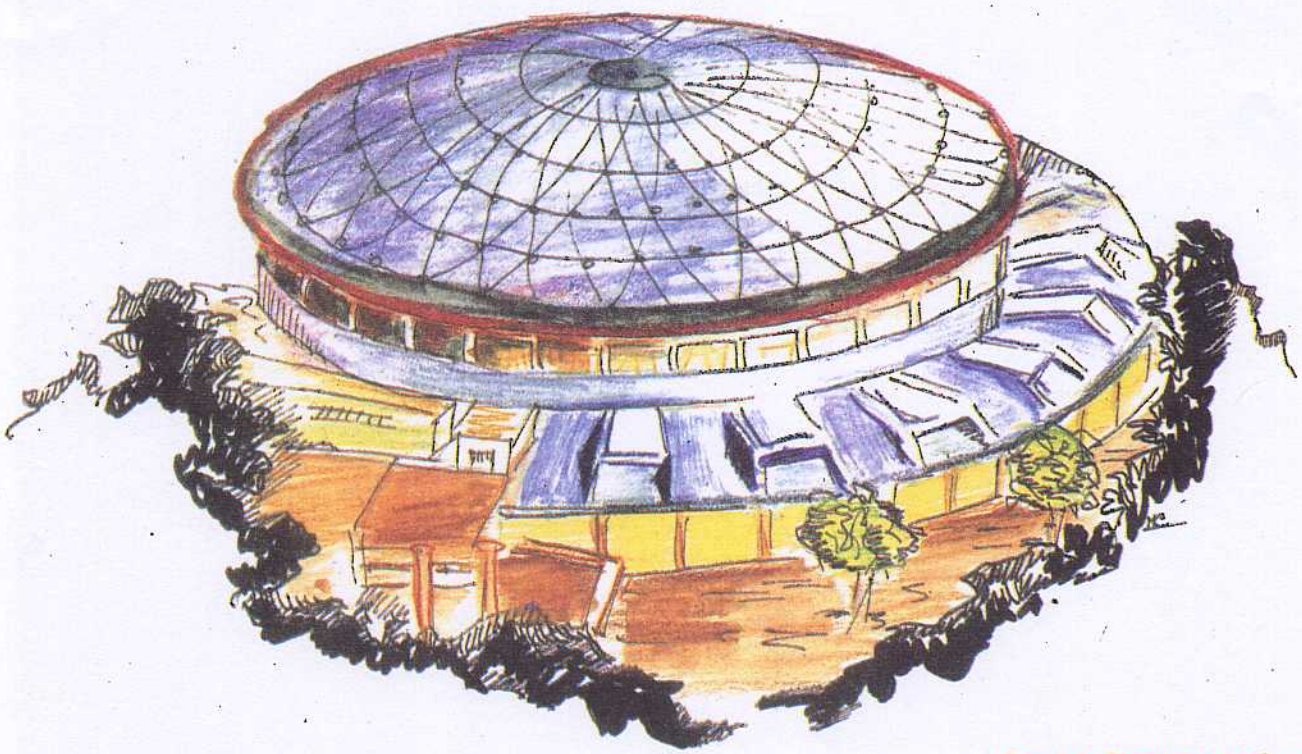

Servizio Documentazione
dei Laboratori Nazionali di Frascati
P.O. Box, 13 - 00044 Frascati (Italy)

LNF-92/084 (P)
4 Novembre 1992

A. Courau, G. Pancheri:

TWO PHOTON CONTRIBUTION TO THE PROCESS $e^+e^- \to e^+e^- \pi\pi$

Contribution to the DAΦNE Physics Handbook

INFN - Laboratori Nazionali di Frascati
Servizio Documentazione

LNF-92/084 (P)
4 Novembre 1992

Two Photon Contribution to the process $e^+e^- \to e^+e^-\pi\pi$

A.Courau[a], G.Pancheri [b]

[a]Laboratoire de L'Accelerateur Lineaire, Orsay, France

[b]INFN,Laboratori Nazionali di Frascati, Frascati, Italy

1 Introduction

e^+e^- machines allow for the measurement and observation of a purely quantum mechanical process like scattering of light by light, in which the photon acts not just as a beam and a probe as in deep inelastic scattering, but also as a target.

The process which allows for the observation of photon-photon scattering is shown in Fig.1, with the notation used throughout this section.

From the point of view of hadronic spectroscopy, photon photon scattering is interesting since it complements the investigations of all the states which are coupled directly to one photon, i.e. states for which $J^{PC} = 1^{--}$ and which proceed through the usual annihilation process [1, 2, 3, 4, 5]. Indeed since the two photon state is C=+1 state, photon photon scattering gives direct access to the study of $J^{PC} = 0^{\pm+}, 2^{\pm+}$. One can thus study the spectroscopy of scalar and pseudoscalar mesons, and of their radiative width, as it has been the case for the pseudoscalars, i.e. π^0, η and η'[6]. The scalar sector is less well known, and it would be very interesting if in the near future we could

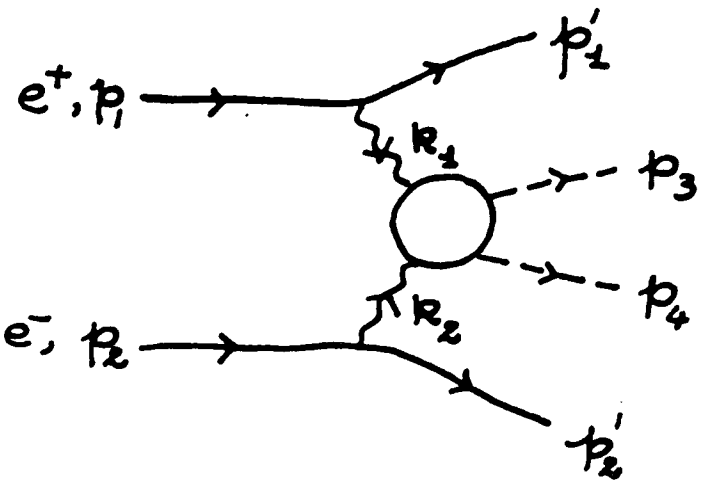

Figure 1: Photon-photon scattering through electron-positron collisions

reach some definitive conclusions regarding the parameters of the low-lying scalar states 0^{++}.

One would expect that the portion of phase space which can be accessed at a machine with $2E \approx 1\ GeV$ to be rather small. As it turns out, however, it will cover a region of great theoretical interest, i.e. the threshold region for the reaction

$$\gamma\gamma -> \pi^0\pi^0 \tag{1}$$

through which one can test, as discussed later in this report [7], the loop structure of chiral lagrangian theories[8, 9, 10].

To study the feasibility of photon-photon experiments at Daphne in the threshold region[11], we shall start by discussing kinematics and luminosity of the gamma gamma system and then examine which is the region accessible to experiments and the machine luminosity needed for a precision measurement[12, 13, 14].

There are two general remarks worth making, from the start :

1. in $\gamma\gamma$ experiments at e^+e^- machines, the photons have a continuous energy and q^2 spectra; both $q_\gamma^2 \approx 0$ as well as $q_\gamma^2 \neq 0$ can be explored.

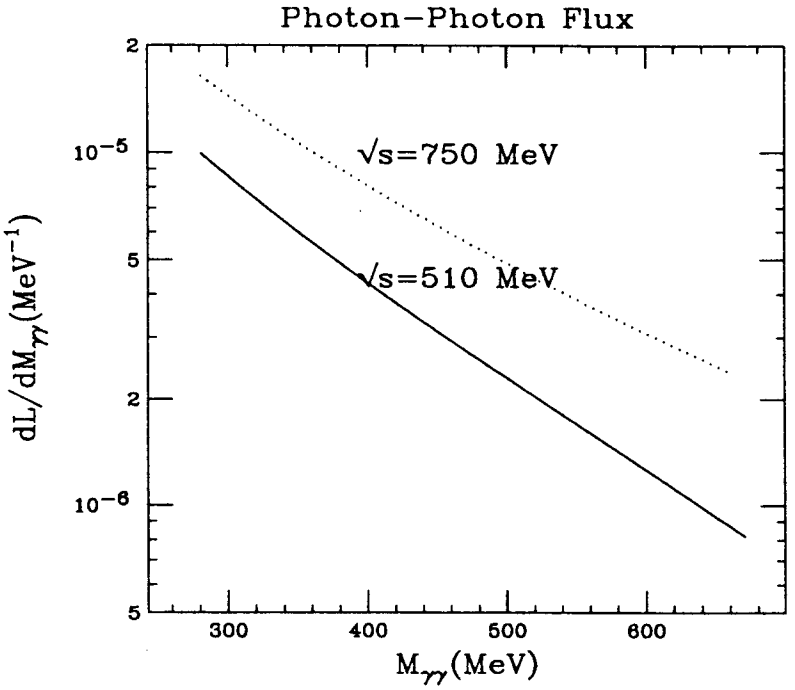

Figure 2: Photon-photon flux at DAΦNE

2. for $q_\gamma^2 \approx 0$ the number of events can be estimated from the expression

$$N = L_{ee} \int \frac{dL_{\gamma\gamma}}{dW_{\gamma\gamma}} \hat{\sigma}(\gamma\gamma \rightarrow final\ state)\ \epsilon\ dW_{\gamma\gamma} \tag{2}$$

where L_{ee} is the machine luminosity, $\frac{dL_{\gamma\gamma}}{dW_{\gamma\gamma}}$ the photon-photon flux, ϵ the detection efficiency, $\hat{\sigma}$ the cross-section into a given final state. As discussed in more detail later, integrating over the full phase space, the photon-photon flux in the double equivalent photon approximation (E.P.A.) is given by [2]

$$\frac{dL_{\gamma\gamma}}{dW_{\gamma\gamma}} = \frac{4}{W_{\gamma\gamma}}(\frac{\alpha}{\pi} ln \frac{E}{m_e})^2[(2+z^2)^2 ln\frac{1}{z} - (1-z^2)(3+z^2)] \tag{3}$$

where E is the beam energy,$W_{\gamma\gamma}$ the photon-photon center of mass energy and $z = \frac{W_{\gamma\gamma}}{2E}$. This function is plotted in Fig.2 for two possible beam energies at DAΦNE.

Integrating over $300 \leq W \leq 600\ MeV$, we get the $\gamma\gamma$ luminosity given by

$$L_{\gamma\gamma/ee} = L_{ee} \int_{300MeV}^{600MeV} \frac{dL_{\gamma\gamma}}{dW_{\gamma\gamma}} dW_{\gamma\gamma} \approx 1.5 \times 10^{-3} L_{ee} \tag{4}$$

Assuming for simplicity a constant cross-section for the subprocess $\gamma\gamma \rightarrow$ *hadrons*, with $\hat{\sigma}(\gamma\gamma \rightarrow \pi^0\pi^0) \approx 5\ nb$[15] and an integrated machine luminosity of $5 \times 10^6 nb^{-1}$, one obtains $\approx$ 40000 events, for an (unrealistic) 100 % detection efficiency. With the same luminosity, the number of events collected in the annihilation process at the ϕ-resonance peak is 10^5 times larger.

These rough estimates are based on kinematics and luminosity functions which we are now going to discuss.

2 Kinematics for head-on collision of two almost real photons

We consider the process

$$\gamma(k_1) + \gamma(k_2) \rightarrow \pi(p_3) + \pi(p_4) \tag{5}$$

In the e^+e^- center-of-mass frame, i.e. in the laboratory frame, let the two photons have the following kinematics :

$$k_1^\mu = \frac{\sqrt{s}}{2}(x_1, 0, 0, x_1) \tag{6}$$

$$k_2^\mu = \frac{\sqrt{s}}{2}(x_2, 0, 0, -x_2) \tag{7}$$

$$p_3^\mu = (E_3, \vec{p_t}, p_3 cos\theta_3) = (m_t chy_3, \vec{p_t}, m_t sinhy_3) \tag{8}$$

$$p_4^\mu = (E_4, -\vec{p_t}, p_4 cos\theta_4) = (m_t coshy_4, -\vec{p_t}, m_t sinhy_4) \tag{9}$$

where $m_t^2 = \mu^2 + p_t^2$ (μ is the pion mass) . In the two photon center-of-mass the particles' momenta are written as

$$k_1^\mu = \frac{\sqrt{\hat{s}}}{2}(1, 0, 0, 1) \tag{10}$$

$$k_2^\mu = \frac{\sqrt{\hat{s}}}{2}(1, 0, 0, -1) \tag{11}$$

$$p_3^\mu = (E^*, \vec{p_t}, p^* cos\theta^*) = (m_t chy^*, \vec{p_t}, m_t sinhy^*) \quad (12)$$

$$p_4^\mu = (E^*, -\vec{p_t}, -p^* cos\theta^*) = (m_t coshy^*, -\vec{p_t}, -m_t sinhy^*) \quad (13)$$

with $\hat{s} = (k_1 + k_2)^2 = s x_1 x_2 = W^2$. The fractional photon energies $x_{1,2}$ are related to the transverse mass m_t and the lab rapidities $y_{3,4}$ through the relations

$$x_1 = \frac{2m_t}{\sqrt{s}}(e^{y_3} + e^{-y_4}) = \frac{2m_t}{\sqrt{s}} coshy_2 \; e^{y_1} \quad (14)$$

$$x_2 = \frac{2m_t}{\sqrt{s}}(e^{-y_3} + e^{y_4}) = \frac{2m_t}{\sqrt{s}} coshy_2 \; e^{-y_1} \quad (15)$$

with $y_{1,2} = \frac{y_3 \pm y_4}{2}$. The rapidities y_1 and y_2 are respectively the rapidity of the center-of-mass of the two photon system in the Laboratory and the rapidity of either pion in their c.m.. This follows easily from the relations

$$P^\mu = (k_1 + k_2)^\mu = \frac{\sqrt{s}}{2}(x_1 + x_2, 0, 0, x_1 - x_2) = (2m_t coshy_2 coshy_1, 0, 0, 2m_t coshy_2 sinhy_1) \quad (16)$$

and $\hat{s} = 4m_t^2 cosh^2 y_2$. Changing notation to

$$Y = y_1 = rapidity\ of\ C.M.\ in\ the\ Lab \quad (17)$$

$$y^* = y_2 = rapidity\ of\ either\ pion\ in\ their\ C.M. \quad (18)$$

$$y_{3,4} = rapidity\ of\ either\ pion\ in\ the\ Lab \quad (19)$$

we have the following set of useful kinematical relations :

$$z^2 = \frac{\hat{s}}{s} = \left(\frac{W}{2E}\right)^2 = \frac{4m_t^2}{s} cosh^2 y^* = x_1 x_2$$
$$Y = tanh^{-1}(\beta) = tanh^{-1}\frac{x_1 - x_2}{x_1 + x_2} = \frac{1}{2} ln \frac{x_1}{x_2} \quad (20)$$

so that

$$y^* = tanh^{-1}(\beta^* cos\theta^*) \qquad \beta^* = \sqrt{1 - \frac{4\mu^2}{\hat{s}}}$$
$$y_{3,4} = tanh^{-1}(\beta_{3,4} cos\theta_{3,4}) \quad with\ y_{3,4} = Y \pm y^* \quad (21)$$

where $\beta_{3,4}$, β^*, $\cos\theta_{3,4}$ and $cos\theta^*$ are respectively velocity and cosine of scattering angle of either pion in the Laboratory and in the C.M., with E the beam energy.

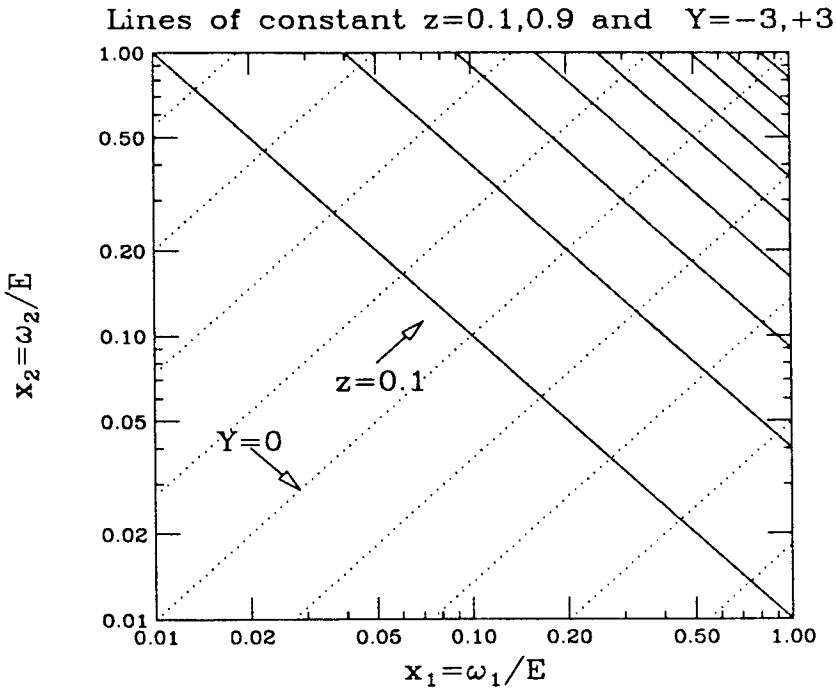

Figure 3: Relations between x_1 and x_2

Sets of independent variables are equally constituted by x_1, x_2 and Y, z. The relations between these two sets are plotted in Fig.3.

In general the detector acceptance puts constraints on the pions' rapidity, i.e. a limited angular acceptance in the Laboratory becomes a rapidity cut on both pions. In fact, assume a cut such that $|y_{3,4}| \leq y_0$ has been imposed. Then since $y_{3,4} = y* \pm Y$, it follows that also $y*, Y \leq y_0$, i.e. $cos\theta* \leq cos\theta_0$, where θ_0 is the angular cut in the Laboratory frame. This is however not the case for $\pi\pi$ production at DAΦNE, for which the limitation on the rapidity Y is due to phase space. For the KLOE detector, in fact, acceptance in the scattering angle of the final state pions is practically the full steradiant, i.e. $cos\theta_0 = 0.98$, which in turn implies $y_0 = 2.29$. On the other hand, since $Y \leq ln\frac{1}{z}$ and $z \geq 0.3$, final state pions will only be emitted with rapidity less than $y_{max} = ln\frac{1}{2\mu} = 1.2$, which corresponds to $cos\theta_0 = 0.85$. In summary, for $\pi\pi$ production at DAΦNE, the limit on rapidity is given by the phase space, as long as the acceptance is larger than $cos\theta_0 = 0.85$. It should also be noticed that the acceptance considerations are valid for two prong events.

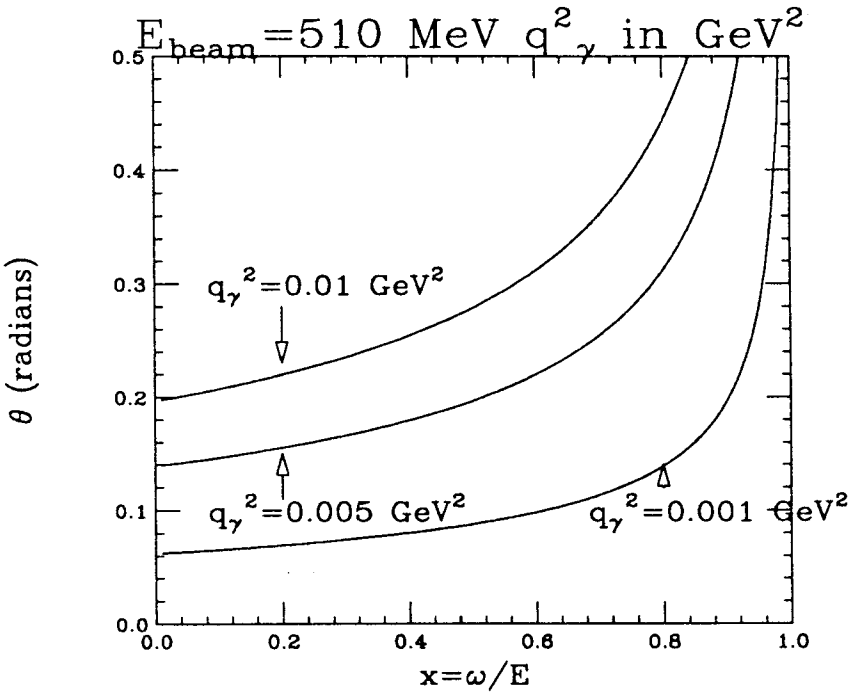

Figure 4: The relation between the electron scattering angle and the photon energy for different values of q_γ^2.

The situation changes somewhat for a four prong event like $\pi^0\pi^0$.

For the general case of virtual photons, we define the following measurable quantities

$$\begin{aligned} E &= initial\ e^+e^-\ energy \\ E_1', E_2' &= final\ e^+\ or\ e^-\ energy \\ \theta_1, \theta_2 &= final\ e^+\ or\ e^-\ polar\ angle \\ \phi_1, \phi_2 &= final\ e^+\ or\ e^-\ azimuthal\ angle \end{aligned} \tag{22}$$

and the following related photon energies

$$\begin{aligned} &\omega_{1,2} = E - E_{1,2}' = Ex_{1,2}\ for\ each\ photon \\ &q_1^2 = -(p_1' - p_1)^2,\ q_2^2 = -(p_2' - p_2)^2\ absolute\ value\ photon\ momenta\ squared \\ &q_{1,2}^2 \approx 2EE_{1,2}'(1 - cos\theta_{1,2}) + m_e^2\frac{\omega_{1,2}^2}{E_{1,2}'E} \\ &W_{\gamma\gamma} = \sqrt{4\omega_1\omega_2 - q_2^2E_1'/E} \quad for\ q_1^2 << q_2^2, m_e << E \end{aligned} \tag{23}$$

The relations between q_1^2, x_1 and θ_1 are shown in Fig.4. Notice that in what follows we shall put $W = W_{\gamma\gamma}$.

3 Cross-Sections and Luminosity

The amplitude for the reaction shown in Fig.1 can be written as

$$A = \frac{e^2}{q_1^2 q_2^2} j_\mu^{(1)} j_\nu^{(2)} T^{\mu\nu} \tag{24}$$

where j_μ's are the electromagnetic currents of the electrons and the tensor $T^{\mu\nu}$ is related to the $\gamma\gamma$ helicity amplitudes through

$$T_{\lambda_1,\lambda_2} = \epsilon^{(1)\mu}(\lambda_1)\epsilon^{(2)\nu}(\lambda_2) T_{\mu\nu} \tag{25}$$

where $\epsilon^{(i)}(\lambda_i)$ is the polarization vector for photon 1 or 2 for a given helicity $\lambda_i = \pm 1$. In a later section, we discuss the gamma gamma amplitude in the helicity basis, here we are primarily concerned with the gamma gamma luminosity. In principle the photons emitted by the electrons will be in a state of transverse (T) or longitudinal (L) polarization and the cross section for process 1, is written as

$$\begin{aligned} d\sigma = \frac{d^3\vec{p_1}}{E_1'}\frac{d^3\vec{p_2}}{E_2'} L_{TT}(\sigma_{TT} + \epsilon_1\sigma_{TL} + \epsilon_2\sigma_{LT} + \epsilon_1\epsilon_2\sigma_{LL} + \\ \frac{1}{2}\epsilon_1\epsilon_2 cos(2\phi)\rho_{TT} + 2\sqrt{\epsilon_1(1+\epsilon_1)}\sqrt{\epsilon_2(1+\epsilon_2)}cos(\phi)\rho_{TL}) \end{aligned} \tag{26}$$

with σ's being the transverse and logitudinal polarization cross-sections, ρ's the interference terms, the polarization coefficients ϵ_i's are functions of the particles' momenta, and ϕ is the azimuthal angle between the outgoing electrons. For most experimental situations, $\epsilon_i \approx 1$ so that the cross-section takes the simple form

$$\frac{d\sigma}{\frac{d^3\vec{p_1}}{E_1'}\frac{d^3\vec{p_2}}{E_2'}} = L_{TT}(\sigma_{TT} + \sigma_{TL} + \sigma_{LT} + \sigma_{LL} + \frac{1}{2}cos(2\phi)\rho_{TT} + 4cos(\phi)\rho_{TL}) \tag{27}$$

A further simplification obtains for the case in which the photons are almost real. Since for real photons only transverse polarization states are allowed, experimentally we must select events with $\frac{q^2}{W^2}$ small so that theoretically we can neglect all longitudinal components which involve q^2/W^2 factors. Then only σ_{TT} and ρ_{TT} will survive. The two terms σ_{TT} and ρ_{TT} are linear

combination of the two helicity amplitudes for real photon scattering. Thus a measument of the azimuthal angle ϕ will allow for a determination of the two amplitudes. We shall comment again in later sections on the theoretical interest for this process and on its feasibility at DAΦNE.

After integration over the azimuthal angle, and for no azimuthal asymmetry, also ρ_{TT} will disappear and the cross section will become

$$d\sigma = \int_{electrons\ angles} \hat{\sigma}_{\gamma\gamma} L_{\gamma\gamma} \frac{d^3\vec{p_1'}}{E_1'} \frac{d^3\vec{p_2'}}{E_2'} \tag{28}$$

where $L_{\gamma\gamma}$ is related to the photon spectrum. In particular, one has that a given counting rate in a variable y is then written as

$$\frac{dN}{dy} = L_{ee} \frac{d\sigma}{dy}(ee \to eeX) = \frac{dL_{\gamma\gamma}}{dy} \sigma(\gamma\gamma \to X) \tag{29}$$

where L_{ee} is the machine luminosity. The photon-photon luminosity function $\frac{dL_{\gamma\gamma}}{dy}$ contains the photon fluxes from the incoming electron beams, and it is a function of the beam energy, the photon fractional momenta and the electron scattering angles. In the double equivalent photon photon approximation, neglecting all q^2/W^2 terms and integrating over ϕ, the luminosity function is given by

$$\frac{1}{L_{ee}} \frac{dL_{\gamma\gamma}}{dx_1 dx_2 dQ_1^2 dQ_2^2} = \frac{N(x_1, Q_1^2)}{x_1} \frac{N(x_2, Q_2^2)}{x_2} = \tag{30}$$

where

$$N(x, Q^2) dQ^2 = \frac{\alpha}{\pi} \frac{dQ^2}{Q^2} \left[1 - x + \frac{x^2}{2} - (1-x) \frac{Q^2_{min}}{Q^2} \right] \tag{31}$$

with $Q^2 = \frac{q^2}{E^2}$ and $Q^2_{min} = Q^2(\theta = 0) = \frac{m_e^2 x^2}{E^2(1-x)}$. This expression has no energy dependence and is dimensionless. The beam energy dependence will arise through the integration limits. Before discussing them, let us illustrate briefly other expressions which can be found in the literature and discuss their use.

An expression often encountered for the luminosity[13] is obtained from the Weiszacker Williams approximation and is given by

$$\frac{1}{L_{ee}} \frac{dL_{\gamma\gamma}}{dx_1 dx_2 d\theta_1 d\theta_2} = \frac{N(E, x_1, \theta_1)}{x_1} \frac{N(E, x_2, \theta_2)}{x_2} = \tag{32}$$

where

$$N(E,x,\theta) = \frac{2\alpha}{\pi}(sin\theta)x^2(1-x)\frac{1}{Q^4}\left[\frac{Q^2}{2} + \frac{(1-x)^2}{x^2+Q^2}sin^2\theta\right] \qquad (33)$$

having already integrated over the azimuthal angle and where θ is the electron's scattering angle. This expression has the disadvantage of using a set of variables, x,Q^2 and θ, which are not independent from each other. By making a small angle approximation ($cos\theta \approx 1$), the above spectrum can then be written as

$$N(E,x,\theta)d\theta = N(x,Q^2)dQ^2 = \frac{\alpha}{\pi}\frac{dQ^2}{Q^2}[\frac{x^2}{2} + (1-x)(1-\frac{Q^2_{min}}{Q^2})\frac{x^2}{x^2+Q^2}] \quad (34)$$

which coincides with eq.(31) if one sets $\frac{x^2}{x^2+Q^2} \simeq 1$, as requested by the equivalent photon approximation, where one explicitely neglects terms of order $Q^2/z^2 \approx Q^2/x^2$.

4 Integrated Photon Spectrum

Let us now discuss the integration of the single photon spectrum. To calculate the number of electrons scattered within a given angle θ, the expression in eq.(31) is integrated between Q^2_{min} and Q^2_{max}. For $\theta = 0$, the lower limit corresponds to

$$Q^2_{min} = \frac{m_e^2x^2}{E^2(1-x)} \qquad (35)$$

whereas for $\theta \neq 0$ one can neglect terms of order m_e/E and write $Q^2 = (1-x)t^2$ with $t = 2sin\frac{\theta}{2}$. Therefore the integration over θ from 0 to θ_{max} corresponds to an integration over Q^2 from Q^2_{min} to $Q^2_{max} = (1-x)t^2_{max}$. One has

$$\int_0^{\theta_{max}} N(x,Q^2)dQ^2 = S(x,\theta_{max}) = \frac{\alpha}{\pi}\cdot$$
$$\left((1+(1-x)^2)ln(\frac{E}{m_e}\frac{1-x}{x}t_{max}) - (1-x)\left[1-\left(\frac{m_ex}{E(1-x)t_{max}}\right)^2\right]\right) \qquad (36)$$

with $t_{max} = 2sin(\frac{\theta_{max}}{2})$. In the small angle limit, we can write

$$S(x,\theta_{max}) = \frac{\alpha}{\pi}\left[(1+(1-x)^2)ln(\frac{E}{m_e}\frac{1-x}{x}\theta_{max}) - (1-x)(1-\left(\frac{m_e x}{E(1-x)\theta_{max}}\right)^2)\right] \tag{37}$$

or, for $(m_e/E)^2 << [(1-x)\theta)/x)]^2$,

$$S(x,\theta_{max}) = \frac{\alpha}{\pi}\left[(1+(1-x)^2)ln(\frac{E}{m_e}\frac{1-x}{x}\theta_{max}) - (1-x)\right] \tag{38}$$

Let us now add a few remarks concerning the range of validity of eq.(37). The quasi reality condition involved in the E.P.A.is that Q^2 is negligible with respect to W^2/E^2. When that condition is satisfied, so that we can neglect the mass of the quasi-real photon, one has

$$x sin\theta_\gamma = (1-x)sin\theta_e \qquad for\ q_\gamma^2 \approx 0 \tag{39}$$

Since $sin\theta_\gamma \leq 1$, it means that for almost real photons one has $sin\theta_e \leq \frac{x}{1-x}$. Therefore one must set

$$S(x,\theta_{max}) = \frac{\alpha}{\pi}\left[(1+(1-x)^2)ln(\frac{E}{m_e}\eta_M) - (1-x)(1-(\frac{m_e}{E\eta_M})^2)\right] \tag{40}$$

with

$$\eta_M = min(1, \frac{1-x}{x}\theta_{max}) \tag{41}$$

We show this spectrum in Fig.5 for various values of the angle θ_{max}, over which the electron's polar angle is being integrated. These curves give the photon spectrum, for the case in which all electrons scattered within an angle θ_{max} are collected.

The quasi real γ-spectrum integrated over the full Q^2, θ allowed range is given by

$$S(x) = \frac{\alpha}{\pi}\left[(1+(1-x)^2)ln(\frac{E}{m_e}\eta_0) - (1-x)(1-(\frac{m_e}{E\eta_0})^2)\right] \tag{42}$$

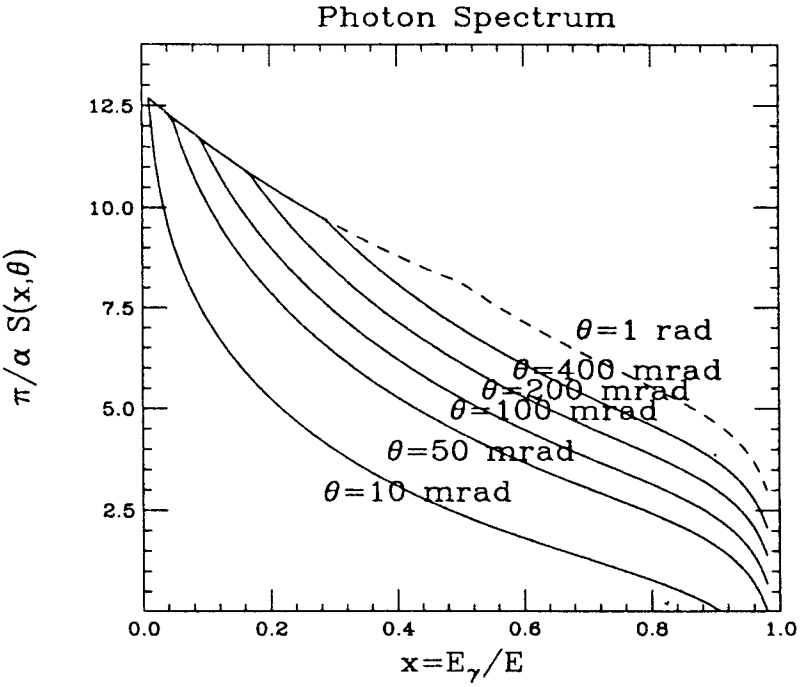

Figure 5: Photon spectrum for different angles of the scattered electron, from eq.(40).

with

$$\eta_0 = min(1, \frac{1-x}{x}) \tag{43}$$

Using. eqs.(40) and (42), one obtains the probability of observing an electron scattered within an angle θ . This normalized γ spectrum is shown in Fig.6, for a set of values of the electron scattering angle θ.

The cut-off we are imposing here, obviously involves the neglect of the contribution of highly virtual photons, the contribution of which remains small and will be overevaluated when extrapolating E.P.A. in this range. Let us also notice that the precise value of this cutoff is generally not very relevant since the $\frac{E}{m}$ factor in the logarithmic term is the dominant one. For small x, eq.(40) reduces to the expression often found in the literature

$$S(x, \theta_{max}) = \frac{\alpha}{\pi}\left[(1+(1-x)^2) ln(\frac{E}{m_e}) - (1-x)\right] \tag{44}$$

i.e. $\eta_0 = 1$. This is a good approximation for high energy (PEP,PETRA,LEP) machines, but is not well adapted to the DAΦNE situation, where x is quite

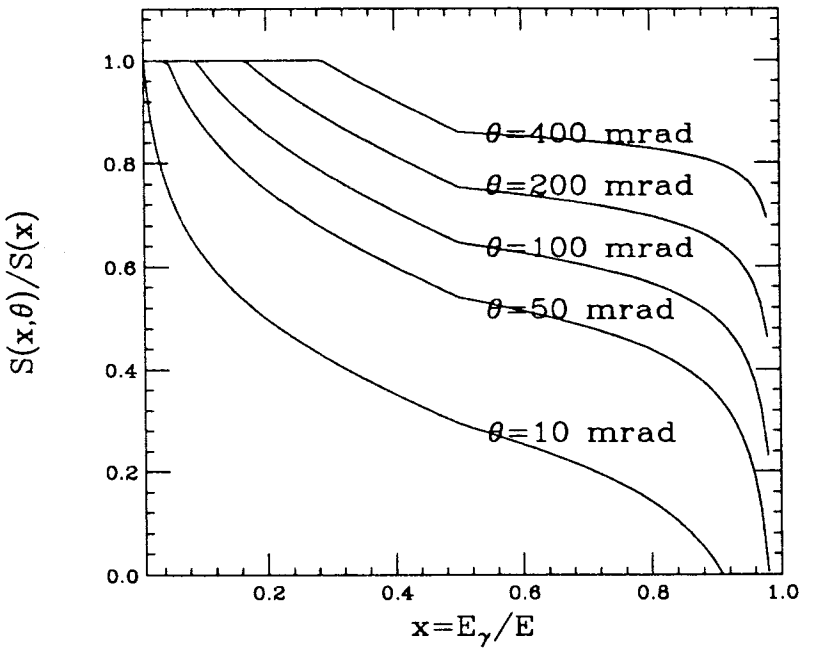

Figure 6: Normalized photon spectrum for different values of the electron scattering angle θ.

large, at least for $\pi\pi$ measurement.

To evaluate the so called 'tagging' efficiency, one can integrate the spectrum over the polar angle θ between θ_{min} and θ_{max}. For $\theta_{min} \leq \theta \leq \theta_{max}$, one gets

$$\bar{S}(x, \theta_{max}, \theta_{min}) = S(x, \theta_{max}) - S(x, \theta_{min}) \approx \frac{\alpha}{\pi}\left[1 + (1-x)^2\right] ln\frac{t_{max}}{t_{min}} \quad (45)$$

with $t_m = min(\frac{x}{1-x}, \theta_m)$. In Figs.7and 8 we plot this function for a set of values $(\theta_{min}, \theta_{max})$. Notice that this function is zero at x=0 and that it is independent of the beam energy E.

The probability of finding a photon of energy E_γ when the electron has been scattered to an angle between θ_0 and θ_{max} is then obtained by normalizing the difference $\bar{S}(x, \theta_{max}, \theta_{min})$ to the full spectrum S(x). We show this probability in Figs.9 and 10.

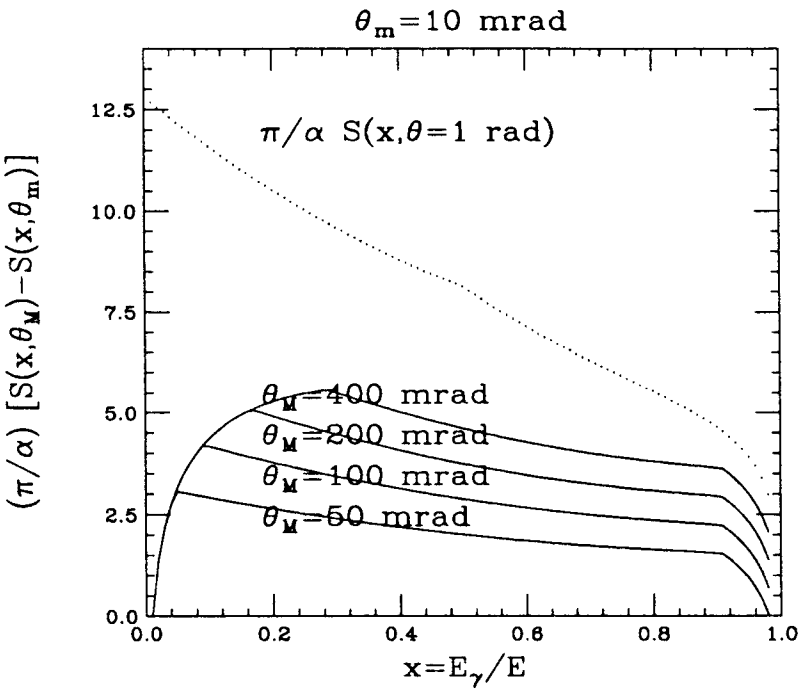

Figure 7: Photon Spectrum, from eq.(40), for electrons scattered between $\theta_m = 10$ *mrad* and θ_M.

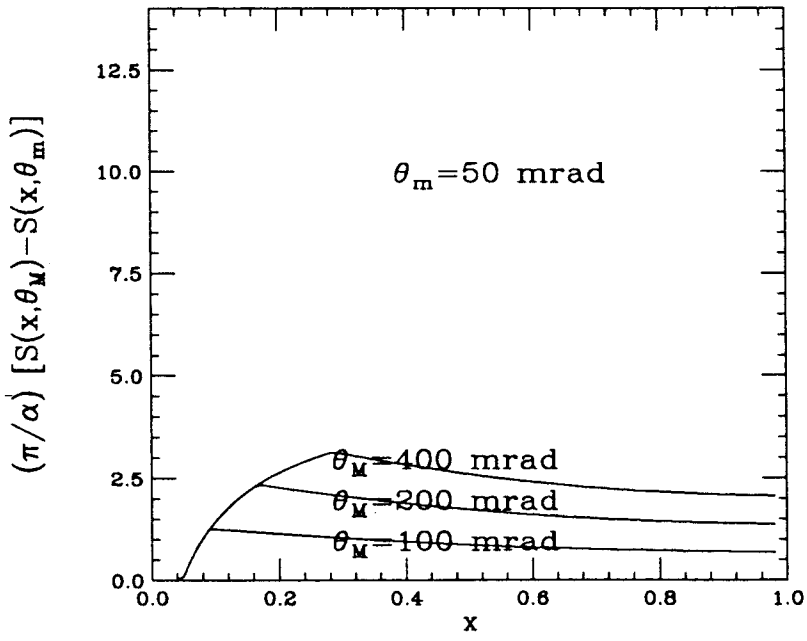

Figure 8: Photon Spectrum, from eq.(40), for electrons scattered between $\theta_m = 50$ *mrad* and θ_M.

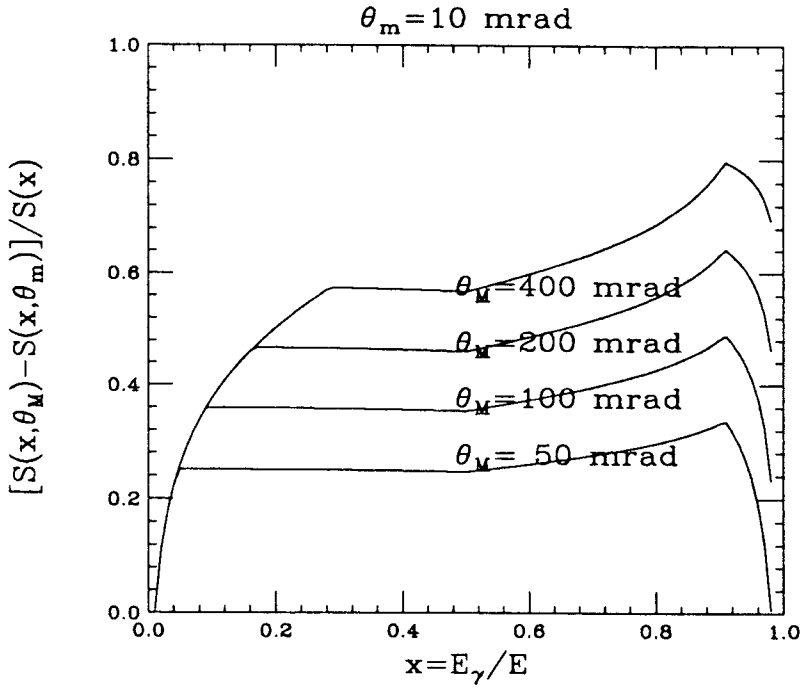

Figure 9: Normalized photon spectrum for electrons scattered between $\theta_{min} = 10$ mrad and $\theta_{max} = 50, 100, 200, 400$mrad.

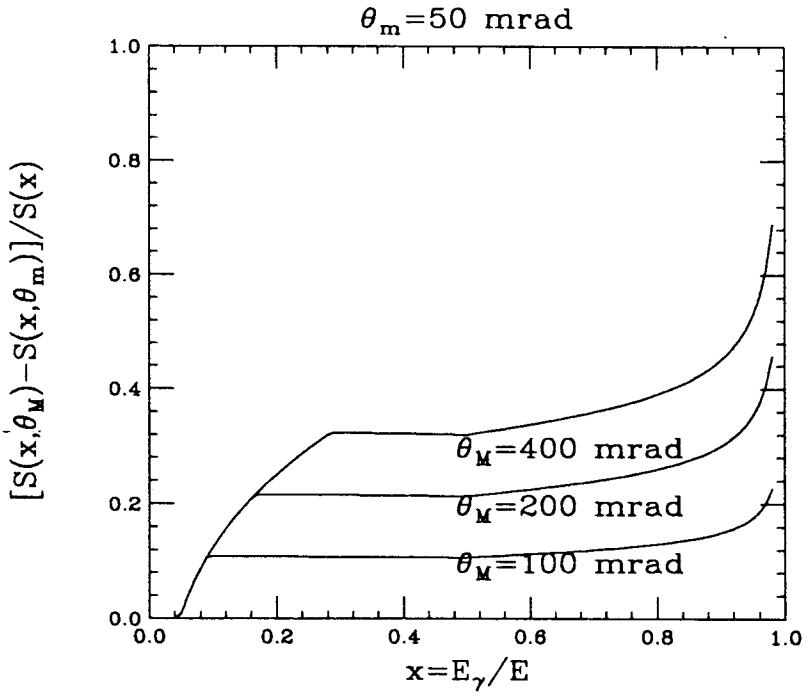

Figure 10: Normalized photon spectrum for electrons scattered between $\theta_{min} = 50$ mrad and $\theta_{max} = 100, 200, 400$mrad.

4.1 Other Approximations

Notice that, had one used eq.(33) rather than eq.(31) for the differential luminosity, one would have obtained

$$\int_0^{\theta_{max}} N(E,x,\theta)d\theta = \frac{\alpha}{\pi}[(1+(1-x)^2)(log\frac{E\theta_{max}}{2m_e}-\frac{1}{2})+ \tag{46}$$

$$+\frac{x^2}{2}(log\frac{2(1-x)}{x}+1)+\frac{(2-x)^2}{2}log\frac{2(1-x)}{\sqrt{x^2+(1-x)\theta_{max}^2}}] \tag{47}$$

which coincides with eq.(37) for $\frac{1-x}{x}\theta_{max} << 1$.

Similarly, for the tagging efficiency, the expression we have used is very close to the one obtained from eq.(33),i.e.

$$N(x,\theta_{min},\theta_{max}) = \\ \frac{\alpha}{\pi}\left[(1+(1-x)^2)log\frac{\theta_{max}}{\theta_{min}}-\frac{(2-x)^2}{4}log\frac{x^2+(1-x)\theta_{max}^2}{x^2+(1-x)\theta_{min}^2}\right] \tag{48}$$

Notice that for small x values, the probability of finding an electron between θ_0 and θ_{max} is often aproximated with the very simple form

$$\Pi_{max}(\theta,\theta_0) = log\frac{\theta_{max}}{\theta_0}/log\frac{2E}{m_e} \tag{49}$$

Finally, an expression often found in the literature[2] is the one for the fully integrated spectrum, i.e.

$$N(\omega) = \int_{-1}^{1} d\theta N(E,x,\theta) = \\ \frac{\alpha}{\pi}\left[\frac{E^2+E'^2}{E^2}(ln\frac{E}{m_e}-\frac{1}{2})+\frac{(E-E')^2}{2E^2}(ln\frac{2E'}{E-E'}+1)+\frac{(E+E')^2}{2E^2}ln\frac{2E'}{E+E'}\right] \tag{50}$$

which corresponds to the one integrated in Q^2 for $Q^2_{max} = 4EE'$.

5 Photon-Photon Luminosity Expressions for untagged experiments

Knowing the expression of the Equivalent Photon Spectra (E.P.S.) integrated over Q^2 , or θ_e, as we did in the previous section, one can define

$$\frac{d\sigma}{dx_1 dx_2 d\Omega *} = \frac{d^2 L_{\gamma\gamma}}{dx_1 dx_2} \frac{d\sigma^{\gamma\gamma\to\pi\pi}(W,\Omega^*)}{d\Omega^*} \tag{51}$$

with

$$\frac{d^2 L_{\gamma\gamma}}{dx_1 dx_2} = \frac{S(x_1)}{x_1}\frac{S(x_2)}{x_2} \tag{52}$$

where S(x) is the *total* E.P.S. (integrated over the whole Q^2 or θ_e range). Then, for x not too close to 1, one gets

$$S(x) = \frac{\alpha}{\pi}\left[2(1-x+\frac{x^2}{2})ln\frac{E}{m_e} - (1-x)\right] \tag{53}$$

which we can approximate with

$$S(x) = \frac{\alpha}{\pi}\left[1+(1-x)^2\right]\left[ln\frac{E}{m_e} - \frac{1}{2}\right] \tag{54}$$

so as to have

$$\frac{d^2 L_{\gamma\gamma}}{dx_1 dx_2} = \left(\frac{\alpha}{\pi}\right)^2 P(x_1,x_2)\left(ln\frac{E}{m_e} - \frac{1}{2}\right)^2 \tag{55}$$

Changing variables from x_1, x_2 to z, Y, one gets

$$\frac{d^2 L_{\gamma\gamma}}{dz dY} = 2\left(\frac{\alpha}{\pi}\right)^2 \frac{P(z,Y)}{z}\left(ln\frac{E}{m_e} - \frac{1}{2}\right)^2 \tag{56}$$

with

$$P(z,Y) = [1+(1-ze^Y)^2][1+(1-ze^{-Y})^2] \tag{57}$$

$$P(z,Y) = 4(1-zcoshY)^2 + z^2(2coshY - z)^2 \tag{58}$$

Now, integrating $P(z,Y)dY$ over $|Y| \leq y_L$, one has

$$H(z,y_L) = 2\int_0^{y_L} P(z,Y)dY = 2[(z^2+2)^2 y_L - 4z(z^2+2-zcoshy_L)sinhy_L] \tag{59}$$

Therefore, integrating over the whole phase space, so that $|Y| \leq y_s$ where $y_s = ln\frac{1}{z}$, one has

$$H(z, y_s) = 2[(z^2+2)^2 ln\frac{1}{z} - (1-z^2)(3+z^2)] \tag{60}$$

and one then finds the expression previously defined in eq.(3), i.e.

$$\frac{dL_{\gamma\gamma}}{dz} = \left(\frac{2\alpha}{\pi}\right)^2 \left(ln\frac{E}{m_e} - \frac{1}{2}\right)^2 \frac{1}{z}\left[(z^2+2)^2 ln\frac{1}{z} - (1-z^2)(3+z^2)\right] \tag{61}$$

The above expression is the one used to obtain the luminosity function plotted in Fig.2.

However, as long as $z < tan\frac{\theta_0}{2}$, where θ_0 defines the angular acceptance of the two prongs in the laboratory ($|cos\theta_{3,4}| \leq cos\theta_0$), the limit over y is not given by the phase space, but by this acceptance according to $|Y| \leq y_0$, where $y_0 = tanh^{-1}(cos\theta_0)$). We then have

$$H(z, y_0) = (z^2+2)^2 ln\left(\frac{1+cos\theta_0}{1-cos\theta_0}\right) - 8z(z^2 + 2 - \frac{z}{sin\theta_0}\frac{cos\theta_0}{sin\theta_0}) \tag{62}$$

It results in particular that for z small with respect to θ_0 (as was the case for low invariant mass $\pi\pi$ production at PEP and PETRA) one has

$$\frac{dL_{\gamma\gamma}}{dz} \approx (\frac{2\alpha}{\pi})^2 (ln\frac{E}{m_e} - \frac{1}{2})^2 \frac{2}{z} ln\frac{1+cos\theta_0}{1-cos\theta_0} \tag{63}$$

instead of

$$\frac{dL_{\gamma\gamma}}{dz} \approx (\frac{2\alpha}{\pi})^2 (ln\frac{E}{m_e} - \frac{1}{2})^2 \frac{4}{z}(ln\frac{1}{z} - 3) \tag{64}$$

6 Tagged Experiments

The expressions derived in the previous section concerned untagged experiments, for which the outgoing electrons are not detected. They can be extended to tagged experiments rather simply for the case of small angle scattering. Under the condition of validity of the expression

$$S(x, \theta_m, \theta_M) = \frac{2\alpha}{\pi}(1 - x + \frac{x^2}{2}) ln\frac{\theta_M}{\theta_m} \tag{65}$$

one can simply replace $(ln\frac{E}{m_e}-\frac{1}{2})^2$ in eq.(62) with $(ln\frac{E}{m_e}-\frac{1}{2})(ln\frac{\theta_M}{\theta_m})$ for single tagging and with $(ln\frac{\theta_M}{\theta_m})^2$ for double tagging.

It should however be noted that the previous derivations are valid only if the cross-section for the process to be measured in the $\gamma\gamma$ system is a constant, since the actual cross-section in the laboratory is obtained by convoluting the $\gamma\gamma$ luminosity with the elementary cross-section for $\gamma\gamma \rightarrow$ *final state*. One cannot integrate $\frac{d^2L_{\gamma\gamma}}{dzdY}$ over Y independently of $\frac{d\sigma}{d\Omega^*}$, since the acceptance in the center of mass obviously depends on $cos\theta_0$ and Y. From $y = Y - y*$, where $y \leq y_0$, it results that the limit on Y is a function of y^* given by $|Y| \leq y_0 - y^*$ with

$$y_0 - y^* = \frac{1}{2} ln\left(\frac{1+cos\theta_0}{1-cos\theta_0}\frac{1-cos\theta^*}{1+cos\theta^*}\right)$$

Therefore

$$\begin{aligned} H(z, y_0 - y^*) &= (z^2+2)^2 ln\left(\frac{1+cos\theta_0}{1-cos\theta_0}\frac{1-cos\theta^*}{1+cos\theta^*}\right) \\ &- \frac{8z(cos\theta_0 - cos\theta^*)}{sin\theta_0 sin\theta^*}\left[z^2 + 2 - z\frac{1-cos\theta_0 cos\theta^*}{sin\theta_0 sin\theta^*}\right] \end{aligned} \tag{66}$$

and in fact, one has

$$\frac{d\sigma}{dW d\Omega*} = \frac{d\hat{L}_{\gamma\gamma}}{dW}\epsilon(z,\theta^*)\frac{d\sigma}{d\Omega^*} \tag{67}$$

with

$$\frac{d\hat{L}_{\gamma\gamma}}{dW} = \left(\frac{2\alpha}{\pi}\right)^2 \frac{1}{W} \tag{68}$$

$$\epsilon(z,\theta^*) = H(z, y_0 - y^*) \tag{69}$$

One notices that for previous experiments like those at DCI and PEP for example, where $z \approx 10^{-2}$ and $cos\theta_0 \leq 0.6$, one simply had

$$\epsilon(\theta^*) = 4\ ln\left[\left(\frac{1+cos\theta_0}{1-cos\theta_0}\right)\left(\frac{1-cos\theta^*}{1+cos\theta^*}\right)\right] \tag{70}$$

with

$$cos\theta^* < cos\theta_0 \tag{71}$$

The function $\epsilon(\theta^*)$ is seen to be peaked at $cos\theta^* = 0$, and to strongly decrease to reach zero for $cos\theta^* \geq cos\theta_0$. This obviously makes the helicity amplitude analysis from the observed θ^* distribution quite inefficient, since the shape of the latter will reflect more about $\epsilon(\theta^*)$ than that of $\frac{d\sigma}{d\Omega^*}$.

The above remarks concern the case of a two body final state with ultrarelativistic kinematics. For the case of massive final state particles, the relative expressions are discussed in ref.[11], where an intuitive, graphical description of all these effects can also be found.

The situation at DAΦNE can now be summarized as follows :

a) for $y^* \leq y_s$ $\quad (cos\theta^* \leq tanh(ln\frac{1}{z})$ or $tan\frac{\theta^*}{2} \geq z)$

$\epsilon(z, y^*) = H(z, y_s)$, i.e. eq.(59) independent of θ^*;

b) for $Y_s \leq y^* \leq y_0$

$\epsilon(z, y^*) = H(z, y_0 - y^*)$, i.e. espression (65).

7 Cross-Sections : $\gamma\gamma \rightarrow \pi\pi$

In the double E.P.A. the general expression for a cross-section for a given $ee \rightarrow ee + X$ process, in terms of $L_{\gamma\gamma}$ is written as

$$\int d\hat{s}\sigma(\hat{s})L_{\gamma\gamma} \tag{72}$$

(i) Hadronic cross-sections. A model independent estimate of the total hadronic cross-section can be obtained, by assuming

$$\sigma_{had}(\hat{s}) \approx constant = \sigma_0 \tag{73}$$

Then the cross-section can be obtained in closed form through

$$\sigma(ee \rightarrow ee + X) = (\frac{2\alpha}{\pi} ln(\frac{2E}{m_e}))^2 \sigma_0 \int_{\hat{s}_0}^1 \frac{d\hat{s}}{\hat{s}} ln\frac{1}{\hat{s}} \tag{74}$$

as

$$\sigma(ee \rightarrow eeX) = \frac{8\alpha^2}{\pi^2} ln^2(\frac{E}{m}) ln^2(\frac{2E}{M_{min}}) \cdot \sigma_0 \tag{75}$$

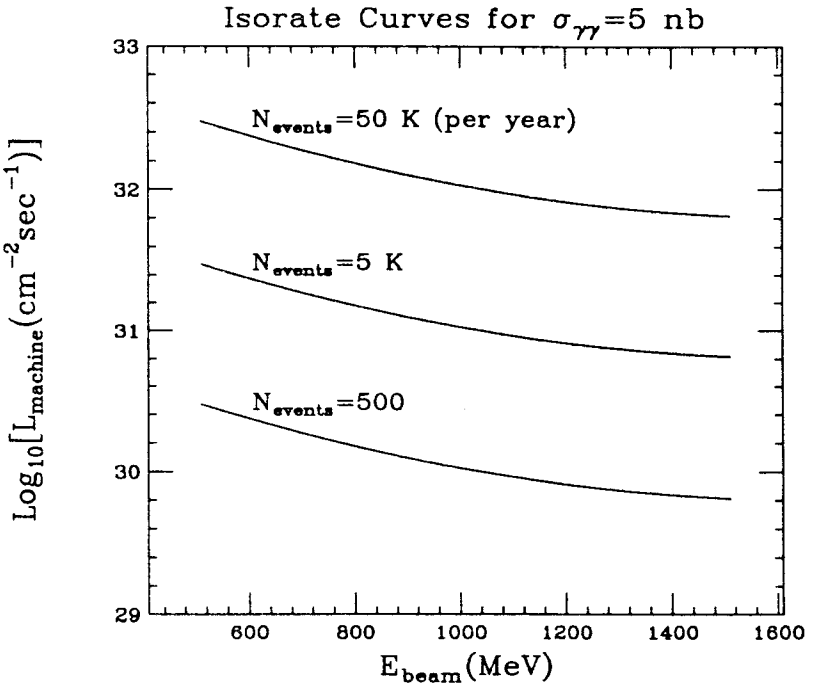

Figure 11: Isorate Curves at DAΦNE

where $\hat{s}_0 = \frac{s_{thresh}}{s}$.

With $\sigma_0 = 5\ nb$, and $s_{thresh} = 4\mu^2$, one obtains a total cross-section of the order of picobarns.

It is a useful exercise to investigate the value of a machine luminosity needed to obtain a typical number of 500 to 500000 events per year at DAΦNE. This is shown in Fig.11 where we see that the present design luminosity ($L \approx 10^{32}$) will allow for a sizable number of events..

We shall now try to be more precise regarding the the photon- photon cross-sections which can be explored. As one can see from Fig.2, the $\gamma\gamma$ luminosity function at DAΦNE decreases very rapidly, almost by a factor 10, as one moves from the 2π threshold to the 4π threshold. This region, $W_{\gamma\gamma} \approx 300 \div 500 MeV$ is precisely the one in which Chiral Perturbation Theory applies and one can use ChPT estimates for this cross-section.

For the process

$$\gamma + \gamma \rightarrow \pi^+ + \pi^- \tag{76}$$

the differential cross-section is calculated to be [9, 10]

$$\frac{d\sigma(W_{\gamma\gamma})}{dcos\theta} = \frac{\pi\alpha^2}{2W_{\gamma\gamma}^2}\beta\left[4|a|^2 - Rea\frac{4\beta^2 sin^2\theta}{1-\beta^2 cos^2\theta} + \frac{4\beta^4 sin^4\theta}{(1-\beta^2 cos^2\theta)^2}\right] \quad (77)$$

where β is the velocity of the pions in the center of mass frame and θ the scattering angle. For $a = 1$, the above expression for the cross-section is simply the Born cross-section, with the well known contribution from the pion pole in the crossed channel [16]. The contribution of Chiral perturbation theory is included for $a \neq 1$, with

$$a = 1 + \frac{4W_{\gamma\gamma}^2}{f^2}(L_9^r + L_{10}^r) - \frac{1}{16\pi^2 f^2}(\frac{3}{2}W_{\gamma\gamma}^2 + \mu^2 ln^2(Q_\pi) + \frac{1}{2}m_K^2 ln^2 Q_K^2) \quad (78)$$

and with

$$Q_i = \frac{\sqrt{W_{\gamma\gamma}^2 - 4m_i^2} + W_{\gamma\gamma}}{\sqrt{W_{\gamma\gamma}^2 - 4m_i^2} - W_{\gamma\gamma}} \quad , f = f_\pi = 134MeV \quad (79)$$

Estimates of the measurability of this cross-section at DAΦNE can be found later in this report [7].

From the point of view of Chiral Perturbation theory, a process of particular interest is also

$$\gamma + \gamma \rightarrow \pi^0 + \pi^0 \quad (80)$$

This process is discussed at length in the following sections of this chapter[7, 17], where comparison between existing measurements [18, 19] and various models can be found, together with an analysis of possible backgrounds and the question of tagging at DAΦNE [20].

(ii) Resonance Production. In photon photon scattering, only states with $J^{PC} = 0^{\pm+}$ and $2^{\pm+}$ can be produced and of these, in the case of DAΦNE, only the J=0 resonant states are kinematically accessible . The cross-section for producing a scalar or pseudoscalar resonance in photon-photon scattering can then be written as

$$\sigma_R = \sigma(\gamma\gamma \rightarrow R \rightarrow final\ state) =$$

$$= \frac{8\pi\Gamma(R \to \gamma\gamma)\Gamma(R \to final\ state)}{(\hat{s} - M_R^2)^2 + M_R^2\Gamma_R^2} \tag{81}$$

where $\Gamma(R \to \gamma\gamma)$ is the resonance decay width into a two photon final state, Γ_R the total decay width. If the narrow width approximation can be used, the above expression folded with the photon luminosities takes the simple form

$$\sigma(ee \to ee + f) = \frac{64\alpha^2}{M_R^3} ln^2(\frac{E}{m_e})\ ln(\frac{2E}{M_R})\Gamma(R \to \gamma\gamma) \tag{82}$$

As far as resonances in the $\gamma\gamma$ system are concerned, at DAΦNE energy and luminosity, there are no narrow $J = 0$ resonances which decay into $\pi's$. Fits of the cross-section with broad enhancement are possible, but then appropriate threshold factors and the Adler's zero must be included in the cross-section. The situation is rather unclear and will be the subject of more in depth study in the future issues of this report.

References

[1] F.E. Low, Phys. Rev. 96 (1954) 1428.

[2] S.Brodsky, T.Kinoshita and H.Terazawa,Phys.Rev.Lett. 25 (1970) 972; S.Brodsky, T.Kinoshita and H.Terazawa,Physical Review D4O (1971) 1532.

[3] V.N.Budnev and I.F.Ginzburg,in Proceedings of the XV International Conference on High Energy Physics (KieV 1970); V.N.Budnev ,I.F.Ginzburg,G.V.Meledin and V.G.Serbo, Physics Rep. 15 (1975)181.

[4] A.Jaccarini,N.Arteaga-Romero, J.Parisi and P.Kessler, Lett. Nuovo Cimento 4 (1970) 933.

[5] M.Greco, Il Nuovo Cimento 4 (1971) 689.

[6] J.K.Bienlein, 'Recent Crystal Ball Results on Resonance Formation in gamma-gamma Reactions', DESY 90-133, November 1990.

[7] S.Bellucci,"Chiral Perturbation Theory Predicts Pion Pion Production via Photon Photon Fusion" in this Chapter.

[8] M.K.Volkov and V.N. Pervushin, 'Description of $\pi\pi$ scattering and the Pion Electromagnetic Properties in Quantum Chiral Field Theory', Nuovo Cimento 27 (1975) 277.
M.V.Terentiev , 'Electromagnetic Properties of Pions at low Energies' Sov.Phys.Usp, 17 (1974)20.

[9] J.F. Donoghue, B.R. Holstein and Y.C. Lin, Phys. Rev. D37 (1988) 2423.

[10] J. Bijnens and F. Cornet, Nucl. Phys. B296 (1988) 557.

[11] A.Courau, 'Gamma Gammma $- >$ $\pi\pi$ near threshold at DAPHNE', Proceeding of the DAPHNE Workshp, Frascati April 1991.

[12] A.Courau, "Tagging and Constraints on $\gamma\gamma$ Experiments" in Proceedings of the International Workshop on $\gamma\gamma$ collisions, Amiens 1984, n.134 of Lecture Notes in Physics, edited by G.Cochard and P.Kessler (Springer-Verlag, New York, 1980) pag.20; Phys. Rev. Lett.49 (1982) 963; Phys. Rev.D 29 (1984)24.

[13] G.Barbiellini, A.Benvenuti, K.Berkelman, A.Courau, F.Foster, K.-W.Lai, F.Lobkowicz, J.Matthews, N.Mistry and T.Rhoades,Proceedings of the 1975 PEP Summer Study, Report N.LBL-4800/SLAC 190,1975,PEP-203, pg.159.

[14] Ch.Berger and W.Wagner' Photon Photon Reactions', Physics Reports 146 (1987) 1.

[15] CELLO Collaboration,'Study of Multihadronic Final States in Photon-photon Interactions', DESY 91-006, February 1991;The CRYSTAL BALL Collaboration, Phys.Rev.D 41 (1990)3324.

[16] H.D.I.Abarbanel and M.Goldberger, ' Low-Energy Theorems, Dispersion Relations and Superconvergence Sum Rules for Compton Scattering', Phys. Rev. 165 (1968)1594.

[17] M.R.Pennington, "Predictions for $\gamma\gamma \rightarrow \pi\pi$: What Photons at DA$\Phi$NE Will See", in this Chapter; D. Morgan and M.R. Pennington, Phys. Lett. 192B (1987) 207 ; Z. Phys. C37 (1988) 431; Z. Phys. C48 (1990) 623; D.Morgan and M.R.Pennington, Phys. Lett. B272 (1991)134.

[18] J.Boyer et al.,"Two Photon Production of Pion Pairs", Phys.Rev. D 42 (1990) 1350. The MARKII Collaboration.

[19] H. Marsiske et al., "A Measurement of $\pi^0\pi^0$ Production in two-photon Collisions" Phys. Rev. D41 (1990) 3324, The CRYSTAL BALL Collaboration.

[20] F.Anulli, D.Babusci, R.Baldini, M.Bassetti, S.Bellucci, G.Matone, G.Pancheri and A.Zallo, "On the Measurements of $\gamma\gamma \rightarrow \pi^0\pi^0$ at DAΦNE", in this Chapter.